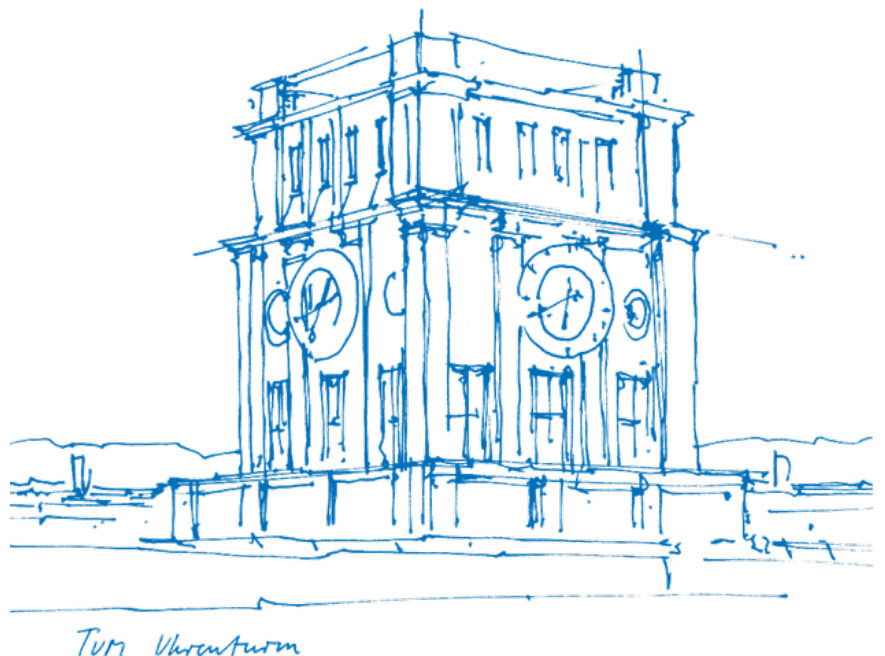


Towards Efficient Helper Data Algorithms for Multi-Bit PUF Quantization

Marius Drechsler



Towards Efficient Helper Data Algorithms for Multi-Bit PUF Quantization

Marius Drechsler

Thesis for the attainment of the academic degree

Bachelor of Science (B.Sc.)

at the School of Computation, Information and Technology of the Technical University of Munich.

Examiner:

Prof. Dr. Georg Sigl

Supervisor:

M.Sc. Jonas Ruchti

Submitted:

Munich, 22.07.2024

Contents

1. Introduction	6
1.1. Notation	7
1.1.1. Tilde-Domain	7
1.1.1.1. ECDF	8
2. S-Metric Helper Data Method	9
2.1. Background	9
2.1.1. Distribution Independency	9
2.1.2. Two-Metric Helper Data Method	9
2.1.3. S-Metric Helper Data Method	11
2.2. Implementation	11
2.2.1. Enrollment	12
2.2.2. Reconstruction	14
2.2.2.1. Offset properties	16
2.3. Improvements	17
2.4. Helper data volume	18
2.5. Experiments & Results	18
2.5.1. General Interpretation	18
2.5.2. Impact of temperature	19
2.5.2.1. Different reconstruction temperature	19
2.5.2.2. Different enrollment temperature	19
2.5.3. Gray coding	19
Glossary	20
Bibliography	21

1 Introduction

These are the introducing words

1.1 Notation

To ensure a consistent notation of functions and ideas, we will now introduce some required conventions

Random distributed variables will be notated with a capital letter, i.e. X , its realization will be the corresponding lower case letter, x .

Vectors will be written in bold test: \mathbf{k} represents a vector of quantized symbols.

We will call a quantized symbol k . k consists of all possible binary symbols, i.e. 0, 01, 110.

A quantizer will be defined as a function $\mathcal{Q}(x, \mathbf{a})$ that returns a quantized symbol k . We also define the following special quantizers for metric based HDAs: A quantizer used during the enrollment phase is defined by a calligraphic \mathcal{E} . For the reconstruction phase, a quantizer will be defined by a calligraphic \mathcal{R}

Figure 1 shows the curve of a 2-bit quantizer that receives \tilde{x} as input. In the case, that the value of \tilde{x} equals one of the four bounds, the quantized value is chosen randomly from the relevant bins.

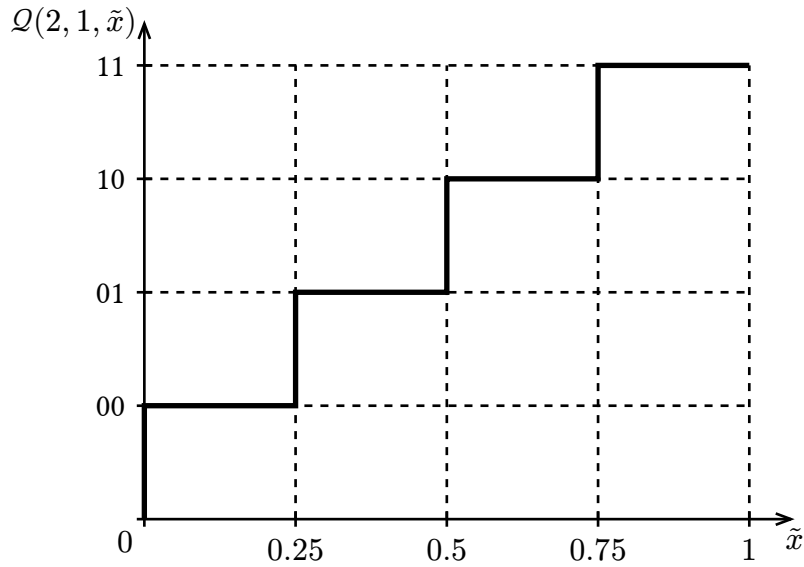


Figure 1: Example quantizer function

For the S-Metric Helper Data Method, we introduce a function

$$\mathcal{Q}(s, m) \tag{1}$$

where s determines the amount of metrics and m the bit width of the symbols.

1.1.1 Tilde-Domain

As also described in [1], we will use a CDF to transform the real PUF values into the Tilde-Domain. This transformation can be performed using the function $\xi = \tilde{x}$. The key property of this transformation is the resulting uniform distribution of x .

Considering a normal distribution, the CDF is defined as

$$\xi\left(\frac{x-\mu}{\sigma}\right) = \frac{1}{2} \left[1 + \operatorname{erf}\left(\frac{x-\mu}{\sigma\sqrt{2}}\right) \right] \quad (2)$$

ECDF

The eCDF is constructed through sorting the empirical measurements of a distribution [2]. Although less accurate, this method allows a more simple and less computationally complex way to transform real valued measurements into the Tilde-Domain. We will mainly use the eCDF in Section 2 because of the difficulty of finding an analytical description for the CDF of a Gaussian-Mixture.

2 S-Metric Helper Data Method

A metric based helper data algorithm (HDA) generates helper data at PUF enrollment to provide more reliable results at the reconstruction stage. Each of these metrics correspond to a quantizer with different bounds to lower the risk of bit or symbol errors during reconstruction.

2.1 Background

2.1.1 Distribution Independency

The publications for the Two-Metric approach [3] and [4], as well as the generalized S-Metric approach [1] make the assumption, that the PUF readout is “zero-mean Gaussian distributed” [1]. We propose, that a Gaussian distributed input for S-Metric quantization is not required for the operation of this quantizing algorithm. Instead, any distribution can be used for input values given, that a CDF exists for that distribution and its parameters are known. As already mentioned in Section 1.1.1, this transformation will result in uniformly distributed values, where equi-probable areas in the real domain correspond to equi-distant areas in the Tilde-Domain. Contrary to [3], [4] and [1], which display relevant areas as equi-probable in a normal distribution, we will use equi-distant areas in a uniform distribution for better understandability. It has to be mentioned, that instead of transforming all values of the PUF readout into the Tilde-Domain, we could also use an inverse CDF to transform the bounds of our evenly spaced areas into the real domain with (normal) distributed values, which can be assessed as remarkably less computationally complex.

2.1.2 Two-Metric Helper Data Method

The most simple form of a metric-based HDA is the Two-Metric Helper Data Method, since the quantization only yields symbols of 1-bit width and uses the lead amount of metrics possible. Publications [3] and [4] find all the relevant bounds for the enrollment and reconstruction phases under the assumption that the PUF readout is Gaussian distributed. Because this approach is static, meaning the parameters for symbol width and number of metrics always stays the same, it is easier to calculate the bounds for 8 equi-probable areas with a standard deviation of $\sigma = 1$ first and then multiplying them with the estimated standard deviation of the PUF readout. This is done by finding two bounds a and b , that

$$\int_a^b f_{X(x)} dx = \frac{1}{8} \quad (3)$$

This operation yields 9 bounds defining these areas $-T1, -a, -T2, 0, T2, a, T1$ and $\pm\infty$. During the enrollment phase, we will use $\pm a$ as our quantizing bounds, retuning 0 if the absolute value is smaller than a and 1 otherwise. The corresponding metric is chosen based on the following conditions:

$$M = \begin{cases} M1, x < -a \vee 0 < x < a \\ M2, -a < x \vee 1 < a < x \end{cases} \quad (4)$$

Figure 2 shows the curve of a quantizer \mathcal{Q} , that would be used during the Two-Metric enrollment phase. At this point, we will still assume, that our input value x is zero-mean Gaussian distributed.

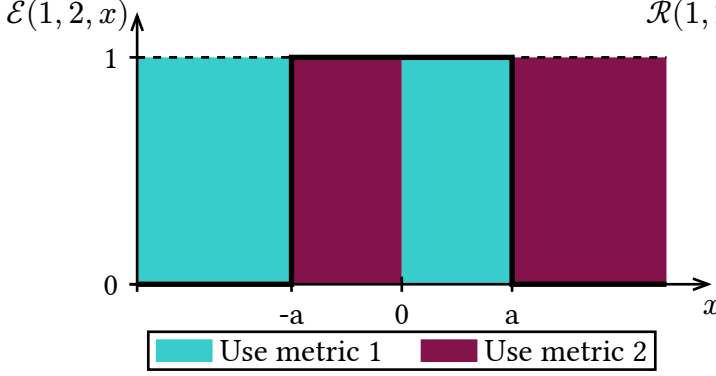


Figure 2: Two-Metric enrollment

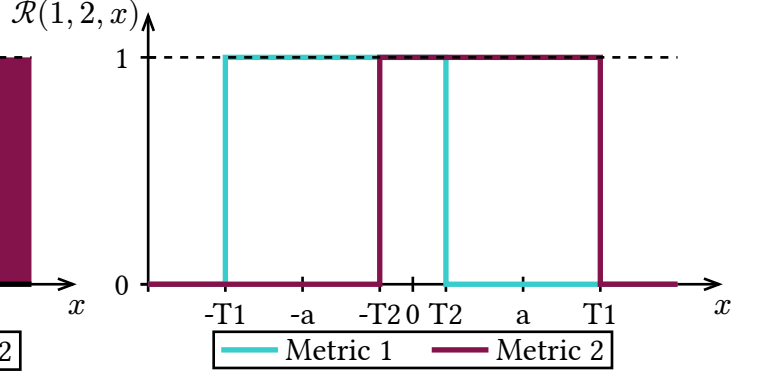


Figure 3: Two-Metric reconstruction

The metric will be stored publicly for every quantized bit as helper data. As previously described, each of these metrics correspond to a different quantizer. Now, we can use the generated helper data in the reconstruction phase and define a reconstructed bit based on the chosen metric as follows:

$$M1 : k = \begin{cases} 0, x < T1 \vee T2 < x \\ 1, -T1 < x < T2 \end{cases} \quad M2 : k = \begin{cases} 0, x < -T2 \vee T1 < x \\ 1, -T2 < x < T1 \end{cases}$$

Figure 3 illustrates the basic idea behind the Two-Metric method. Using the helper data, we will move the bounds of the original quantizer one octile to each side, yielding two new quantizers. The advantage of this method comes from moving the point of uncertainty away from our readout position.

Figure 4 and Figure 5 illustrate an example enrollment and reconstruction process. We would consider the marked point the value of the initial measurement and the marked range our margin of error due to inaccuracies in the measurement process. If we now were to use the quantizer shown in Figure 4 during both the enrollment and the reconstruction phases, we would risk a bit error, because the margin of error overlaps with the lower quantization bound $-a$. But since we generated helper data during enrollment as depicted in Figure 2, we can make use of a different quantizer $\mathcal{R}(1, 2, x)$ whose boundaries do not overlap with the error margin of the measurement.

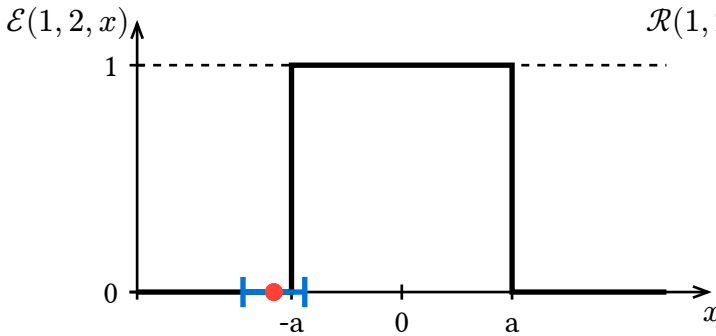


Figure 4: Example enrollment

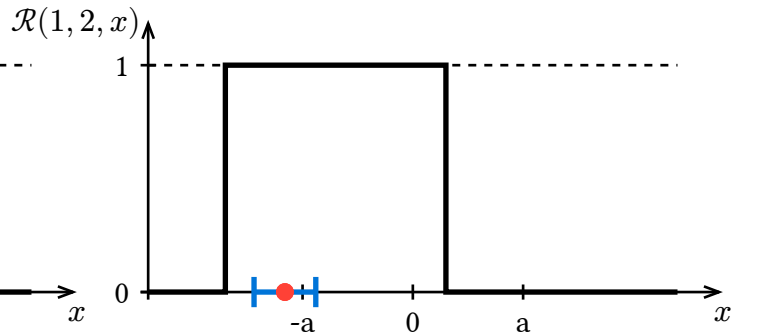


Figure 5: Example reconstruction

2.1.3 S-Metric Helper Data Method

Going on, the Two-Metric Helper Data Method can be generalized as shown in [1]. This generalization allows for higher order bit quantization and the use of more than two metrics.

A key difference to the Two-Metric approach is the alignment of quantization areas. Methods described in [3] and [4] use two bounds for 1-bit quantization, namely $\pm a$. Contrary, the method introduced by [1] would look more like a sign based quantizer if the configuration $\mathcal{Q}(2, 1)$ is used, using only one quantization bound at $x = 0$. Figure 6 and Figure 7 illustrate this difference.

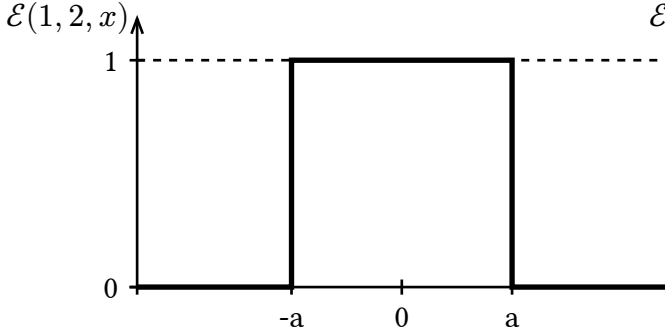


Figure 6: Two-Metric enrollment

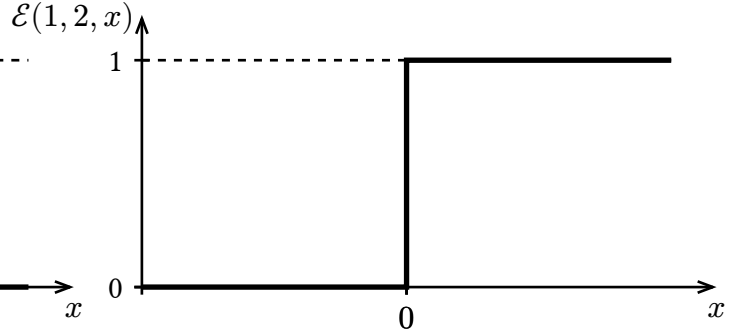


Figure 7: S-Metric enrollment with 1-bit configuration

The generalization consists of two components:

- **Higher order bit quantization**

We can introduce more steps to our quantizer and use them to extract more than one bit out of our PUF readout.

- **Using more than two metrics**

Instead of splitting each quantizer into only two equi-probable parts, we can increase the number of metrics at the cost of generating more helper data.

2.2 Implementation

We will now propose a specific implementation of the S-Metric Helper Data Method.

As shown in Section 2.1.1, we can use a CDF to transform our random distributed variable X into the Tilde-Domain: \tilde{X} . This allows us to use equi-distant bounds for the quantizer instead of equi-probable ones.

From now on we will use the following syntax for quantizers that use the S-Metric Helper Data Method:

$$\mathcal{Q}(s, m, \tilde{x}) \tag{6}$$

where s defines the number of metrics, m the number of bits and \tilde{x} a Tilde-Domain transformed PUF measurement.

2.2.1 Enrollment

To enroll our PUF key, we will first need to define the quantizer for higher order bit quantization and helper data generation. Because our PUF readout \tilde{x} can be interpreted as a realization of a uniformly distributed variable \tilde{X} , we can define the width Δ of our quantizer bins as follows:

$$\Delta = \frac{1}{2^m} \quad (7)$$

For example, if we were to extract a symbol with the width of 2 bits from our PUF readout, we would need to evenly space $2^2 = 4$ bins. Using equation Equation 7, the step size for a 2-bit quantizer would result to:

$$\Delta' = \frac{1}{2^m} \Big|_{m=2} = \frac{1}{4} \quad (8)$$

Figure 8 shows a plot of the resulting quantizer function that would yield symbols with two bits for one measurement \tilde{x} .

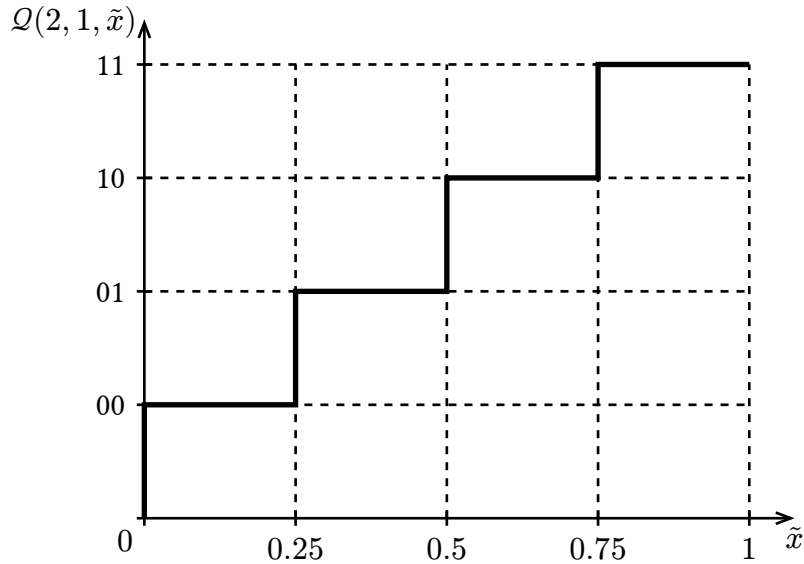


Figure 8: 2-bit quantizer

Right now, this quantizer wouldn't help us generating any helper data. To achieve that, we will need to divide a symbol step - one, that returns the corresponding quantized symbol - into multiple sub-steps. More specifically, we will define the amount of metrics we want to use with the parameter s . Using s , we can define the step size Δ_s as the division of Δ by s :

$$\Delta_s = \frac{\Delta}{s} = \frac{\frac{1}{2^m}}{s} = \frac{1}{2^m \cdot s} \quad (9)$$

After this definition, we need to make an adjustment to our previously defined quantizer function, because we cannot simply return the quantized value based on a quantizer with step size Δ_s . That would just increase the amounts of bits we will extract out of one measurement. Instead, we will

need to return a tuple, consisting of the quantized symbol and the metric ascertained that we will save as helper data for later.

Going on in our example, we could choose the amount of our metrics to be 2. According to Equation 9, we would then half our step size:

$$\Delta'_s = \frac{\Delta'}{s} \Big|_{s=2} = \frac{1}{4 \cdot 2} = \frac{1}{8} \quad (10)$$

This means, we can update our quantizer function with the new step size $\Delta'_s = \frac{1}{8}$ and redefining its output as a tuple consisting of bit value and helper data.

We can visualize the quantizer that we will use during the enrollment phase of a 2-bit 2-metric configuration as depicted in Figure 9.

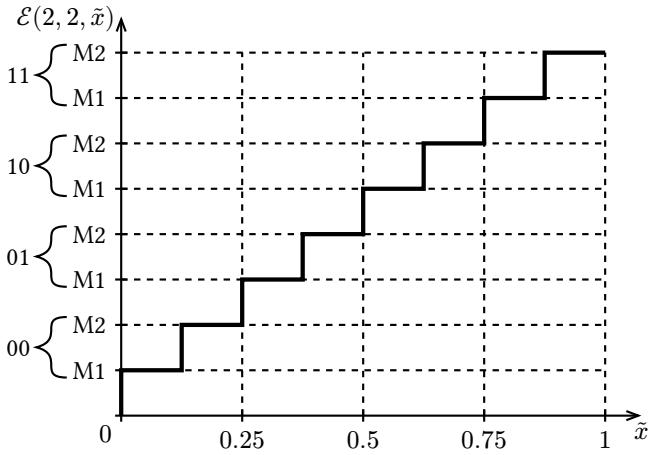


Figure 9: 2-bit 2-metric enrollment

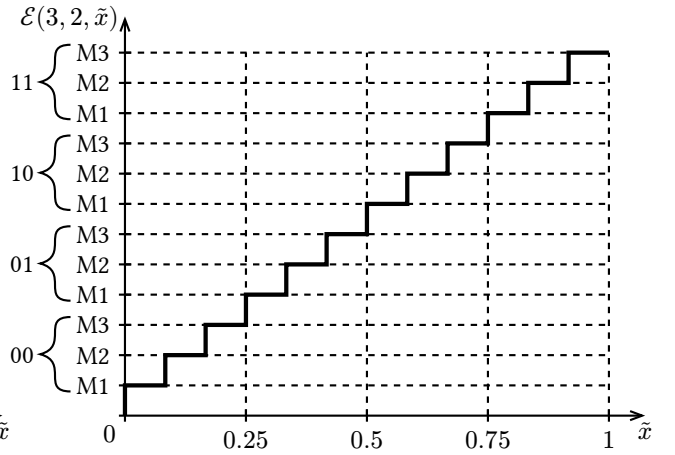


Figure 10: 2-bit 3-metric enrollment

To better demonstrate the generalization to s -metrics, Figure 10 shows a 2-bit quantizer that generates helper data based on three metrics instead of two. In that sense, increasing the number of metrics will increase the number of sub-steps for each symbol.

We can now perform the enrollment of a full PUF readout. Each measurement will be quantized with our quantizer \mathcal{E} , returning a tuple consisting of the quantized symbol and helper data, as shown in Equation 11

$$K_i = \mathcal{E}(s, m\tilde{x}_i) = (k, h)_i \quad (11)$$

Performing the operation of Equation 11 for our whole set of measurements will yield a vector of tuples \mathbf{K} .

2.2.2 Reconstruction

We already demonstrated the basic principle of the reconstruction phase in section Section 2.1.2, more specifically with Figure 4 and Figure 5, which show the advantage of using more than one quantizer during reconstruction.

We will call our repeated measurement of \tilde{x} that is subject to a certain error \tilde{x}^* . To perform reconstruction with \tilde{x}^* , we will first need to find all s quantizers for which we generated the helper data in the previous step.

We have to distinguish two different cases for the value of s :

- s is odd
- s is even

If s is even, we need to move our quantizer $\frac{s}{2}$ times some distance to the right and $\frac{s}{2}$ times some distance to the left. We can define the ideal position for the quantizer bounds based on its corresponding metric as centered around the center of the related metric.

We can find these new bounds graphically as depicted in Figure 11. We first determine the x-values of the centers of a metric (here M1, as shown with the arrows). We can then place the quantizer steps with step size Δ (Equation 7) evenly spaced around these points. With these new points for the vertical steps of \mathcal{Q} , we can draw the new quantizer for the first metric in Figure 12.

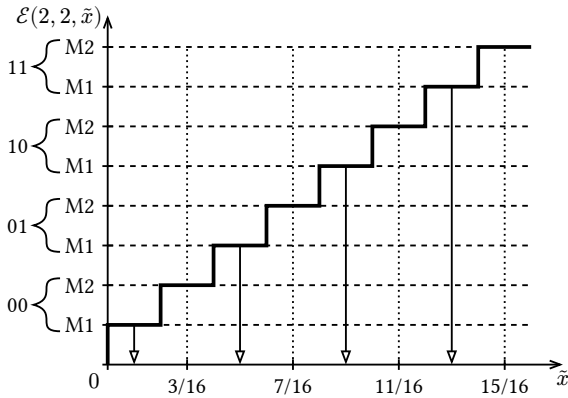


Figure 11: Ideal centers and bounds for the M1 quantizer

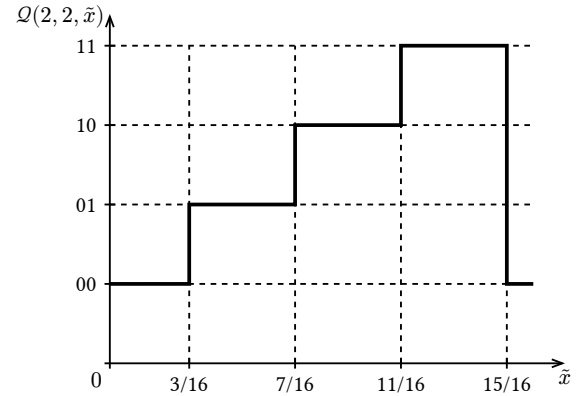


Figure 12: Quantizer for the first metric

As for metric 2, we can apply the same strategy and find the points for the vertical steps to be at $\frac{1}{16}$, $\frac{5}{16}$, $\frac{9}{16}$ and $\frac{13}{16}$. This quantizer can be visualized together with the first metric quantizer in Figure 13, forming the complete quantizer for the reconstruction phase of a 2-bit 2-metric configuration $\mathcal{R}(2, 2, \tilde{x})$.

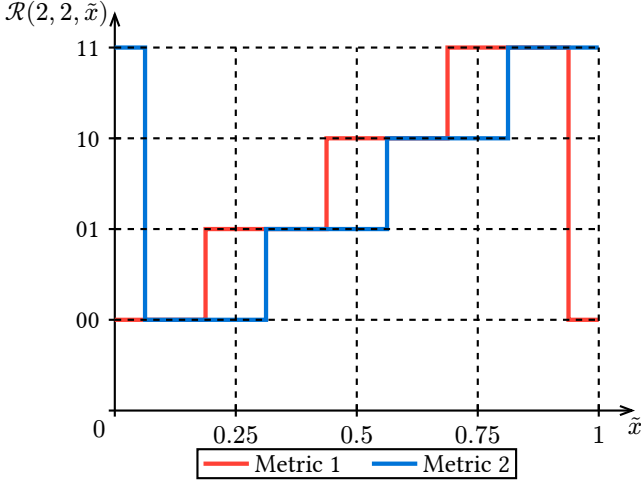


Figure 13: 2-bit 2-metric reconstruction quantizer

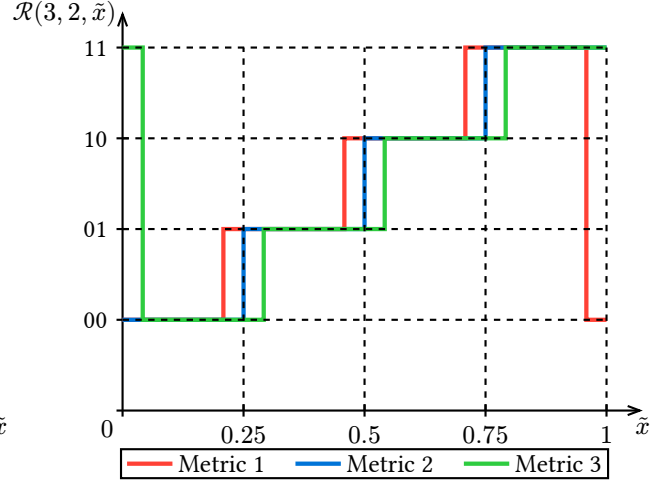


Figure 14: 2-bit 3-metric reconstruction quantizer

Analytically, the offset we are applying to $\mathcal{E}(2, 2, \tilde{x})$ can be defined as

$$\varphi = \frac{1}{2^n \cdot s \cdot 2} \Big|_{n=2, s=2} = \frac{1}{16} \quad (12)$$

This is also shown in Figure 13, as our quantizer curve is moved $\frac{1}{16}$ to the left and the right.

If a odd number of metrics is given, the offset can still be calculated using Equation 12. Additionally, we will keep the original quantizer used during enrollment (Figure 14).

Comparing Figure 13, Figure 14 and their respective values of Equation 12, we can observe, that the offset φ gets smaller the more metrics we use.

m	1	2	3	4	5	6	7	8	9	10
φ	$\frac{1}{8}$	$\frac{1}{16}$	$\frac{1}{24}$	$\frac{1}{32}$	$\frac{1}{40}$	$\frac{1}{48}$	$\frac{1}{56}$	$\frac{1}{64}$	$\frac{1}{72}$	$\frac{1}{80}$

Table 1: Offset values for 2-bit configurations

To find all offsets for values of $s > 3$, we can use Algorithm 1. For application, we calculate φ based on the metric using Equation 12. The resulting list of offsets is correctly ordered and can be mapped to the corresponding metrics in ascending order as we will show in Table 2 and Table 3.

Algorithm 1: Find all offsets

```

1 list offsets
2 if  $s$  is odd
3    $s = s - 1$ 
4   append 0 to list offsets
5 while  $i \leq \frac{s}{2}$ 
6   append  $+(i \cdot \varphi)$  to list offsets
7   append  $-(i \cdot \varphi)$  to list offsets
8 sort list offsets in ascending order
9 end
  
```

Offset properties

Lets look deeper into the properties of the offset value φ . As previously stated, we will need to move the enrollment quantizer $\frac{s}{2}$ times to the left and $\frac{s}{2}$ times to the right. For example, setting parameter s to 4 means we will need to move the enrollment quantizer $\frac{s}{2}|_{s=4} = 2$ times to the left and right. As we can see in Table 2, φ for the indices $i = \pm 2$ are identical to the offsets of a 2-bit 2-metric configuration. In fact, this property carries on for higher even numbers of metrics.

i	-2	-1	1	2
Metric	M1	M2	M3	M4
φ	$-\frac{1}{16}$	$-\frac{1}{32}$	$\frac{1}{32}$	$\frac{1}{16}$

Table 2: 2-bit 4-metric offsets

i	-3	-2	-1	1	2	3
Metric	M1	M2	M3	M4	M5	M6
φ	$-\frac{1}{16}$	$-\frac{1}{24}$	$-\frac{1}{48}$	$\frac{1}{48}$	$\frac{1}{24}$	$\frac{1}{16}$

Table 3: 2-bit 6-metric offsets

At $s = 6$ metrics, the biggest offset we encounter is $\varphi = \frac{1}{16}$ at $i = \pm 3$.

In conclusion, the maximum offset for a 2-bit configuration φ is $\frac{1}{16}$ and we will introduce smaller offsets in between if we use a higher even number of metrics. More formally, we can define the maximum offset for an even number of metrics as follows:

$$\varphi_{\max, \text{even}} = \frac{\frac{s}{2}}{2^n \cdot s \cdot 2} = \frac{1}{2^n \cdot 4} \quad (13)$$

Here, we multiply Equation 12 with the maximum offsetting index $i_{\max} = \frac{s}{2}$.

Now, if we want to find the maximum offset for a odd number of metrics, we need to modify Equation 13, more specifically its numerator. We know, that we need to keep the original quantizer for a odd number of metrics. Besides that, the method stays the same. For that reason, we will decrease the parameter m by 1, that way we will still perform a division without remainder:

$$\varphi_{\max, \text{odd}} = \frac{\frac{s-1}{2}}{2^n \cdot s \cdot 2} \quad (14.1)$$

$$= \frac{s-1}{2^n \cdot s \cdot 4} \Big|_{n=2, s=3} = \frac{1}{24} \quad (14.2)$$

It is important to note, that $\varphi_{\max, \text{odd}}$, unlike $\varphi_{\max, \text{even}}$, is dependent on the parameter s as we can see in Table 4.

s	3	5	7	9
$\varphi_{\max, \text{odd}}$	$\frac{1}{24}$	$\frac{1}{20}$	$\frac{3}{56}$	$\frac{1}{18}$

Table 4: 2-bit maximum offsets, odd

The higher m is chosen, the closer we approximate $\varphi_{\max, \text{even}}$ as shown in Equation 15.1. This means, while also keeping the original quantizer during the reconstruction phase, the maximum offset for an odd number of metrics will always be smaller than for an even number.

$$\lim_{s \rightarrow \infty} \varphi_{\max, \text{odd}} = \frac{s-1}{2^n \cdot s \cdot 4} \quad (15.1)$$

$$= \frac{1}{2^n \cdot 4} = \varphi_{\max, \text{even}} \quad (15.2)$$

2.3 Improvements

The here proposed S-Metric Helper Data Method can be improved by using gray coded labels for the quantized symbols instead of naive ones [1].

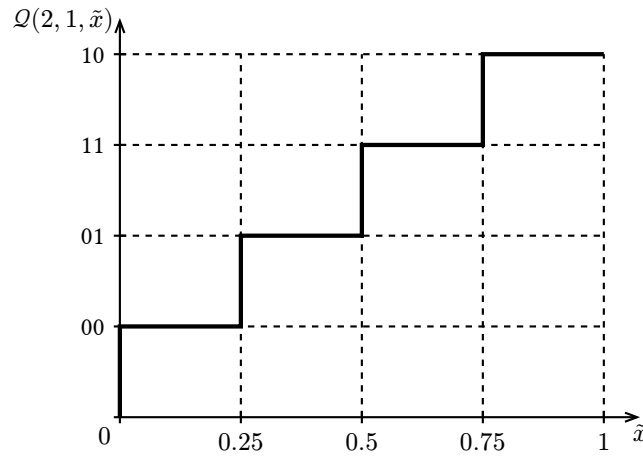


Figure 15: Gray Coded 2-bit quantizer

Figure 15 shows a 2-bit quantizer with gray coded labelling. In this example, we have an advantage at $\tilde{x} = \sim 0.5$, because a quantization error only returns one wrong bit instead of two.

2.4 Helper data volume

2.5 Experiments & Results

We tested the implementation of Section 2.2 with the temperature dataset of [5]. The dataset contains counts of positives edges of a toggle flip flop at a set evaluation time D . Based on the count and the evaluation time, the frequency of a ring oscillator can be calculated using: $f = 2 \cdot \frac{k}{D}$. Because we want to analyze the performance of the S-Metric method over different temperatures, both during enrollment and reconstruction, we are limited to the second part of the experimental measurements of [5]. We will have measurements of 50 FPGA boards available with 1600 and 1696 ring oscillators each. To obtain the values to be processed, we subtract them in pairs, yielding 800 and 848 ring oscillator frequency differences df .

Since the frequencies f are normal distributed, the difference df can be assumed to be zero-mean Gaussian distributed. To apply the values df to our implementation of the S-Metric method, we will first transform them into the Tilde-Domain using an inverse CDF, resulting in uniform distributed values \tilde{df} .

2.5.1 General Interpretation

The bit error rate of different S-Metric configurations for naive labelling can be seen in Figure 16. For this analysis, enrollment and reconstruction were both performed at room temperature and the quantizer was naively labelled.

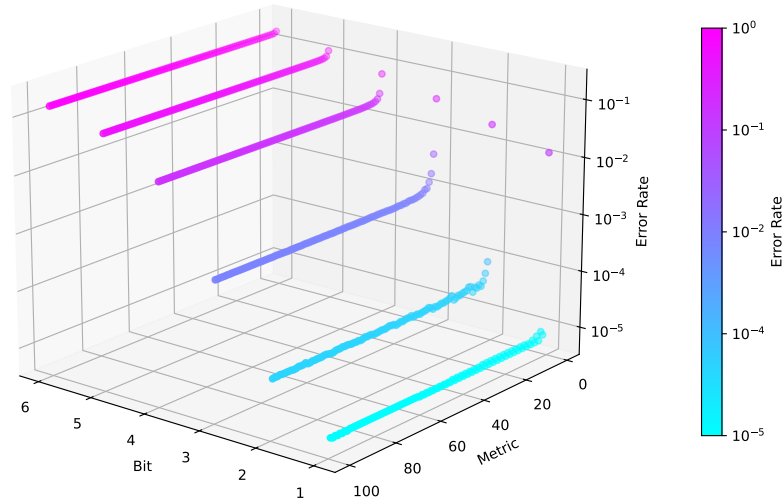


Figure 16: Bit error rates for same temperature execution

We can observe two key properties of the S-Metric method in Figure 16. The error rate in this plot is scaled logarithmically.

The exponential growth of the error rate of classic 1-metric configurations can be observed through the linear increase of the error rates. Also, as we expanded on in Section 2.2.2.1, using more metrics will, at some point, not further improve the bit error rate of the key. At a symbol width of $m \geq 6$ bits, no further improvement through the S-Metric method can be observed.

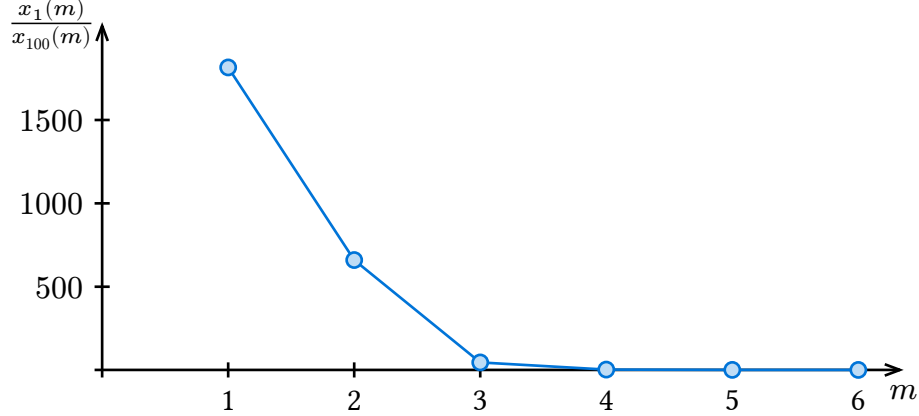


Figure 17: Asymptotic performance of S-Metric

This tendency can also be shown through Figure 17. Here, we calculated the quotient of the bit error rate using one metric and 100 metrics. From $m \geq 6$ onwards, $\frac{x_1(m)}{x_{100}(m)}$ approaches ~ 1 , which means, no real improvement is possible anymore through the S-Metric method.

2.5.2 Impact of temperature

Usually we will perform enrollment at room temperature. We will now take a look at the impact of changing the temperature both during the enrollment and the reconstruction phase.

Different reconstruction temperature

Different enrollment temperature

2.5.3 Gray coding

Glossary

HDA – helper data algorithm. 9

Bibliography

- [1] R. F. Fischer, “Helper Data Schemes for Coded Modulation and Shaping in Physical Unclonable Functions,” *arXiv preprint arXiv:2402.18980*, 2024.
- [2] F. M. Dekking, *A Modern Introduction to Probability and Statistics: Understanding why and how*. Springer Science & Business Media, 2005.
- [3] J.-L. Danger, S. Guilley, and A. Schaub, “Two-metric helper data for highly robust and secure delay PUFs,” in *2019 IEEE 8th International Workshop on Advances in Sensors and Interfaces (IWASI)*, 2019, pp. 184–188.
- [4] L. Tebelmann, U. Kühne, J.-L. Danger, and M. Pehl, “Analysis and protection of the two-metric helper data scheme,” in *International Workshop on Constructive Side-Channel Analysis and Secure Design*, 2021, pp. 279–302.
- [5] R. Hesselbarth, F. Wilde, C. Gu, and N. Hanley, “Large scale RO PUF analysis over slice type, evaluation time and temperature on 28nm Xilinx FPGAs,” in *2018 IEEE International Symposium on Hardware Oriented Security and Trust (HOST)*, 2018, pp. 126–133.